THE ASTROPHYSICAL JOURNAL, 451:L61–L64, 1995 October 1

A PERIOD-LUMINOSITY RELATION FOR THE SLOW VARIATIONS OF LUMINOUS BLUE VARIABLES

RICHARD B. STOTHERS AND CHAO-WEN CHIN
Institute for Space Studies, NASA/Goddard Space Flight Center, 2880 Broadway, New York, NY 10025
Received 1995 May 19; accepted 1995 July 26

ABSTRACT

The slow (annual-to-decadal) cycles of light and color variation displayed by many luminous blue variables show mean "periods" that are inversely proportional to the stars' luminosities. New theoretical evolutionary tracks reveal that very massive stars undergo repeated mass outbursts due to quasi-secular oscillations of the stellar envelope between dynamically stable and unstable states, at the observed locations of LBVs at quiescence in the H-R diagram. Within the estimated errors, the models correctly predict the observed "periods," eruption mass-loss rates, and lack of dependence of these rates on the stars' luminosities. During a cycle the models shift nearly imperceptibly on the H-R diagram. Observed variations of light and color in the LBVs are therefore probably attributable to changes in size of the optically thick ejected cloud. An earlier phase of stronger dynamical instability is predicted to have led to the ejection of huge circumstellar shells, whose computed masses scale with stellar luminosity in roughly the manner observed for massive old nebulae surrounding LBVs.

Subject headings: stars: evolution — stars: oscillations — stars: variables: other

1. INTRODUCTION

Luminous blue variables (LBVs) comprise a class of intrinsically bright stars that display different scales of light and color variability, ranging from rapid microvariations to rare outbreaks of catastrophic mass loss. Most characteristically, LBVs exhibit quasi-regular cycles of annual-to-decadal length with amplitudes of several tenths of a magnitude to ~2 mag in blue light (Hubble & Sandage 1953; Humphreys & Davidson 1994). We have discovered an apparent relation between the mean cycle length and the stellar luminosity for these slow variations, which appear to be due to moderate-sized mass outbursts. Such a relation is useful to have, because LBVs are often employed as standard candles in studies of the extragalactic distance scale. The new relation can be theoretically understood by invoking a recent model of the LBV phenomenon that has already successfully predicted the massive outbursts and the observed locations of the LBVs at quiescence in the Hertzsprung-Russell (H-R) diagram (Stothers & Chin 1993, 1994, hereafter SC93, SC94).

The mechanism that we have found to be responsible for the outbursts is a classical example of dynamical instability. The instability develops in the outer envelope layers of a very massive post–main-sequence supergiant as a result of the effects of high radiation pressure and partial ionization of hydrogen and helium. A necessary auxiliary condition is the near isolation of the outer layers of the envelope, caused by a large iron opacity bump at a temperature of 2×10^5 K. Before the new opacities containing this iron bump (Rogers & Iglesias 1992; Iglesias, Rogers, & Wilson 1992) were utilized in stellar models, no proposed model for a LBV was ever actually found to be dynamically unstable.

Previously proposed mechanisms for LBVs were entirely speculative, having been based on the mild density inversion occurring in the outer convection zone (Bisnovatyi-Kogan & Nadyoshin 1972; Maeder 1989), on an assumed excessive radiation pressure in either the envelope (Stothers & Chin 1983) or the atmosphere (Davidson 1971; Lamers & Fitzpatrick 1988; Appenzeller 1989), or on an assumed very strong turbulent pressure in the atmosphere (de Jager 1984). Our new mechanism is a different phenomenon from the dynamical strange-mode and mode-coupling instabilities discovered by Glatzel & Kiriakidis (1993) and Kiriakidis, Fricke, & Glatzel (1993). Unstable strange modes exist also in the case of the old Los Alamos opacities and occur even during the main-sequence phase of evolution—for stellar masses as low as 20 $M_\odot$. Therefore, we doubt that they are the cause of the cyclic outbursts of the LBVs, although Langer et al. (1994) have recently assumed that they can pulsationally induce mass loss. Perhaps the strange modes and the suggested atmospheric instabilities are responsible for the rapid microvariations seen in LBVs and other luminous blue stars (see, e.g., Abt 1957; van Genderen 1989).

2. EMPIRICAL RELATION BETWEEN MEAN CYCLE LENGTH AND LUMINOSITY

LBVs for which a sufficient number of slow cycles have been observed to estimate a mean cycle length are listed in Table 1. These mean cycle lengths, or "periods," range from 4 to 20 yr. P Cyg displayed a possible 18 yr "period" during its intense seventeenth century activity (Pigott 1786), but the cycles seem to have vanished, or at least to have become inconspicuous, since then (de Groot 1985). Nevertheless, Percy et al. (1988) have rediscovered in recent data some evidence for long-term variations with a possible amplitude of 0.2 mag, and so we include P Cyg in Table 1. Its inclusion or omission is not critical to our conclusions.

Luminosities of the LBVs (Humphreys & Davidson 1994) are also listed in Table 1. They correlate closely with the mean "periods," P, as shown in Figure 1, where the regression line is given by

$$M_{\rm bol} = (-12.9 \pm 0.5) + (2.4 \pm 0.5) \log P,$$

and the standard deviation is 0.3 mag. The faintest members of the LBV class, with $M_{\rm bol} \approx -9$, would accordingly be expected to show "periods" of well over 20 yr. This expectation appears to be confirmed by the fragmentary material available for HR Car, HD 160529, and R71 (Sharov 1975; Spoon et al. 1994).

Notice that the mean "period" decreases with increasing

TABLE 1

SLOW PERIODICITIES OF LUMINOUS BLUE VARIABLES

Variable	Galaxy	M_{bol}	Cycle Lengths (yr)	Adopted P (yr)	References
η Car.....	MW	−11.6:	3–5	4	1, 2, 3
AF And	M31	−11.4:	3–7	5	4, 5, 6
AG Car.....	MW	−10.8:	4–14	9	7, 8
Var. B.....	M33	−10.2	5–8	7	4, 5, 6
P Cyg.....	MW	−9.9	...	18:	9
S Dor.....	LMC	−9.8	10–30	19	8, 10, 11
Var. C.....	M33	−9.8	19–20	20	4, 5, 6, 12

REFERENCES.—(1) Feinstein & Marraco 1974; (2) van Genderen et al. 1994; (3) Whitelock et al. 1994; (4) Hubble & Sandage 1953; (5) Rosino & Bianchini 1973; (6) Sharov 1990; (7) Sharov 1975; (8) Spoon et al. 1994; (9) Pigott 1786; (10) Gaposchkin 1943; (11) van Genderen 1979; (12) Humphreys et al. 1988.

luminosity in accordance with the approximate relation $P \propto L^{-1}$. This is contrary to what might be expected for LBVs as pulsating variable stars: $P \propto L^{-1.8}$, as based on the simple theoretical relations $P \propto M^{-1} R^2$ (Gough, Ostriker, & Stobie 1965), $M \propto L^{0.8}$ (SC94), and $L \propto R^2 T_e^4$, together with the empirical relation $L \propto T_e^2$ (Fig. 2). In fact, the slow "periods" of LBVs are probably incompatible with a pulsational hypothesis. Our nonlinear hydrodynamical calculations for a dynamically unstable LBV model (SC93) confirm that relaxation oscillations occur and grow, but are fairly regular with periods of only months to ~1 yr. Although driven pulsations of the circumstellar shell that is being ejected would show a somewhat longer period and might be less regular (Stothers & Chin 1983), actual observations of LBV shells suggest that the shells' natural oscillation periods are in fact of the order of months (Leitherer et al. 1985; Wolf & Stahl 1990). We, therefore, abandon a pulsational explanation of the long cycles.

3. THEORETICAL LBV MODELS

Evolutionary tracks have been computed here in order to follow the evolution of very massive stars explicitly through their first phase of dynamical instability and into their second phase, where we believe most LBVs reside. As representative

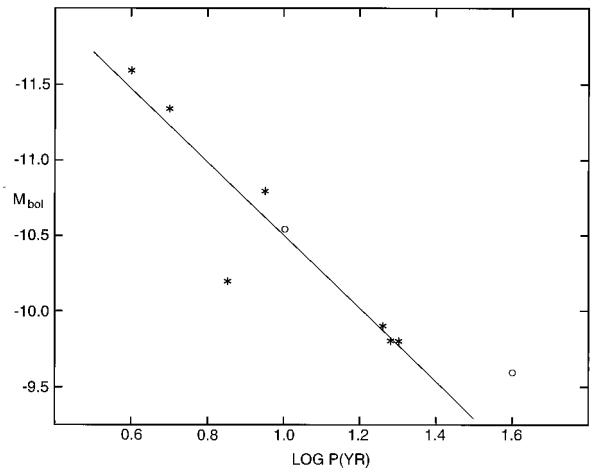

FIG. 1.—Period-luminosity relation for the slow cyclical variations observed in seven LBVs (*asterisks*) and predicted from stellar models evolving in the second phase of dynamical instability (*open circles*). The regression line is fitted only through the observational points.

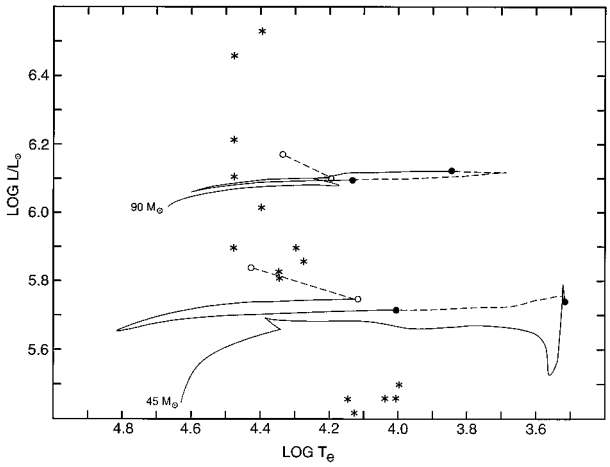

FIG. 2.—H-R diagram showing two evolutionary tracks running from the zero-age main sequence (initial stellar mass indicated) to the locus of the second phase of dynamical instability. Dashed portions of the evolutionary track connect the starting and terminating points of the first phase of dynamical instability (*filled circles*) and of the second phase (*open circles*). Individual cycles during the second phase show unobservably small amplitudes if the effects of the ejected shell are ignored. Locations of observed LBVs at quiescence are also plotted (*asterisks*).

initial stellar masses, we take 45 and 90 $M_\odot$. Stellar wind mass loss is included, as in our previous work, at a rate equal to w times the observationally based expression given by Nieuwenhuijzen & de Jager (1990). Unless stated otherwise, we use $w = 1$. During the quiescent LBV stages, we have adopted the probably more accurate observational rates of 1×10^{-6} and 1×10^{-5} $M_\odot$ yr^{-1} (Lamers 1989) for our evolutionary tracks at 45 and 90 $M_\odot$, respectively. Rates of mass loss used for dynamically unstable stellar models will be described below.

Since evolution up to the start of the second phase of dynamical instability has already been covered in detail (SC94), we simply report here that the stellar remnant resulting from the first phase is found to be relatively insensitive to the assumed rate of dynamically induced mass loss. For our 45 $M_\odot$ sequence, the first phase begins in the red supergiant configuration while the star is depleting core helium (Fig. 2). The stellar mass at this time falls quickly from 22 to 18 $M_\odot$, and the final surface hydrogen abundance, X_{surf}, is 0.20.

The stripped-down star evolves through the remainder of core helium burning as a blue supergiant. When the central helium abundance, Y_c, falls to 0.03 and the surface cools to log $T_e = 4.11$, dynamical instability is encountered again. The resulting sudden loss of mass induces a small, rapid blueward shift, which immediately restabilizes the envelope structure. Then normal evolutionary processes resume and reexpand the envelope, until dynamical instability sets in once again. The result is a sort of quasi-secular oscillation of the star away from a nearly fixed effective temperature, with a small temperature amplitude of 0.012 dex and an even smaller luminosity amplitude of 5×10^{-4} dex.

Our detailed calculations covering many cycles indicate that the mean rate of mass loss during the dynamically unstable portion of the cycle (the eruption phase) must lie in the range $(4-8) \times 10^{-5}$ $M_\odot$ yr^{-1} in order to keep the cycles going. If the mass-loss rate is temporarily too low, the star evolves farther below the threshold effective temperature, becoming more unstable and thereby increasing its mass-loss rate until the amount of mass lost is sufficient to force the star blueward

TABLE 2

MODELS AND OBSERVED VARIABLES ASSIGNED TO THE SECOND PHASE OF DYNAMICAL INSTABILITY

Initial $M/M_\odot$	Model or Variable	w	$M/M_\odot$	X_{surf}	log $(L/L_\odot)$	log T_e	Eruption $\dot{M}$ ($M_\odot$ yr^{-1})	Cycle Lengths (yr)	P (yr)
90	Model	1	34	0.08	6.11	4.19[a]	$\sim 8 \times 10^{-5}$	5–15	10
	Model	0.2	38	0.16	6.13	4.16[a]	$(4–8) \times 10^{-5}$	5–20	10
	AG Car	...	...	...	6.23:	4.48:	$(1–10) \times 10^{-5}$	4–14	9
50	Model[b]	1	21	0.20	5.82	4.19[a]	$(4–8) \times 10^{-5}$	20–40	30
	S Dor	...	23	...	5.82	4.35	$(5–10) \times 10^{-5}$	10–30	19

[a] Start of the second phase.
[b] Interpolated to the same luminosity as that of S Dor.

again. The resulting cycles show lengths of 30–50 yr, with a mean length of 40 yr. The star thus hovers about the border line of dynamical instability until enough mass is expelled to push the star permanently blueward of the line. The time necessary to achieve this is estimated to be $\sim 10^4$ yr. During this time, the instability line becomes somewhat hotter as a result of continuing mass loss and evolutionary brightening of the star.

Turning now to the evolutionary sequence for 90 $M_\odot$, we find that the first phase of dynamical instability occurs when the star is a yellow supergiant, with a contracting helium core and an expanding envelope (Fig. 2). Since the whole star is secularly unstable, it remains so during the brief time that dynamical instability lowers the star's mass from 51 to 36 $M_\odot$, with X_{surf} becoming 0.09. Afterward, the continuing expansion of the envelope leads to recurrent episodes of less violent mass loss around an effective temperature of log $T_e = 4.14$, until the core and envelope finally stabilize under central helium burning. This process takes $\sim 10^3$ yr. Regardless of the assumed rate of dynamically induced mass loss, the same final structure is always obtained.

Helium now begins to deplete in the core of a very blue star, and when Y_c falls below 0.2 the star enters its second phase of dynamical instability. Cycles of eruption, with mean rates of mass loss equal to $\sim 8 \times 10^{-5}$ $M_\odot$ yr^{-1}, occur at an average frequency of one eruption every 10 yr. The full range of derived cycle lengths is 5–15 yr. The effective temperature oscillates away from log $T_e = 4.19$ with a remarkably small temperature amplitude of 0.002 dex and a negligible luminosity amplitude of 3×10^{-5} dex. The total lifetime of this phase is estimated to be $\sim 10^4$ yr.

Since the rates of main-sequence mass loss used here are possibly too high (Lamers & Leitherer 1993), we have adopted $w = 0.2$ in a rerun of the 90 $M_\odot$ sequence (the 45 $M_\odot$ sequence would be hardly affected). The first phase of dynamical instability now occurs when the star is a red supergiant; the star's mass drops quickly from 65 to 40 $M_\odot$, with X_{surf} becoming 0.16. The rest of the evolution is roughly as in the case for $w = 1$.

Toward the end of the second phase of dynamical instability, evolutionary brightening causes the instability to occur at a hotter effective temperature than before. This change of effective temperature leads to some spread in the theoretically predicted locus of the brightest LBVs at quiescence in the H-R diagram.

Table 2 compares our theoretical LBV models with two well-observed stars, AG Car and S Dor. Observational data are taken from Humphreys & Davidson (1994), Wolf & Stahl (1982, 1990), Leitherer et al. (1985), and the listed references in Table 1. Agreement between theory and observation is very close, within the estimated uncertainties.

4. CONCLUSION

Our new models support the idea that most, if not all, LBVs are experiencing recurrent episodes, or cycles, of dynamical instability. These episodes appear at two different evolutionary phases, both of them at times when the stellar envelope is undergoing rapid expansion, viz., (1) shortly after the end of central hydrogen burning and (2) shortly before the end of central helium burning.

The first phase initially leads to an enormous, sudden loss of mass: $\Delta M = 4 \pm 1$ $M_\odot$ for stars with log $(L/L_\odot) = 5.7$, and $\Delta M = 20 \pm 5$ $M_\odot$ for stars with log $(L/L_\odot) = 6.1$, implying $\Delta M \propto L^{1.7 \pm 0.5}$. This predicted relation agrees, at least in slope, with Hutsemékers's (1994) observational relation for massive old nebulae seen around LBVs, $\Delta M \propto L^{1.55 \pm 0.10}$.

If the star's original mass was sufficiently high (>60 $M_\odot$), the first phase of dynamical instability ends with a series of cycles of lesser mass loss until the star stabilizes under the onset of central helium depletion. For a star of smaller initial mass ($\sim 30–60$ $M_\odot$), no such cycles appear, because dynamical instability is first encountered during the middle stages of central helium depletion when the envelope's natural tendency is to shrink (and hence to avoid further dynamical instability).

All luminous single stars with initial masses exceeding ~ 30 $M_\odot$ are expected to enter into the later, and much more prolonged, second phase of dynamical instability, characterized by a lengthy series of moderate mass loss cycles. If the first phase also has such cycles, the cycles of both the first and second phases occur on the H-R diagram in roughly the same place (Fig. 2). The star's interior properties at the two times are not radically different, except for a core helium difference due to an age difference of $(1–3) \times 10^5$ yr. Note that the predicted instability band in the H-R diagram lies close to where the LBVs, corrected for obscuration (Humphreys & Davidson 1994), are actually observed.

During a mass ejection episode the stellar models move hardly at all on the H-R diagram. This seems to be observationally supported in that the large measured light and color variations of LBVs have been generally traced to changes in size of the optically-thick ejected cloud (see, e.g., Davidson 1987; Wolf 1989).

Theoretical and observed eruption mass loss rates agree very well with each other, $(1–10) \times 10^{-5}$ $M_\odot$ yr^{-1}. Both rates are also essentially independent of luminosity (Table 2; Lamers 1989; Humphreys & Davidson 1994).

Predicted lengths of the quasi-regular cycles agree satisfactorily with observations as regards both the total range of

lengths and the average length (Table 2). The mean "period" declines with increasing stellar luminosity owing to the smaller radius excursions experienced by the stars of higher luminosity.

Sometimes a larger than normal outburst occurs in the models. The star then shifts further blueward than normal, and the length of that particular cycle can be centuries rather than years to decades. P Cyg is characterized by $M/M_\odot = 23 \pm 2$, $\log (L/L_\odot) = 5.86 \pm 0.10$, $\log T_e = 4.28 \pm 0.02$, and $d(\log T_e)/dt = -0.027 \pm 0.004$ century^{-1} since its last great outburst three centuries ago (Pauldrach & Puls 1990; Lamers & de Groot 1992). Interpolation among our models to match the luminosity and effective temperature of P Cyg yields theoretically expected values of $M/M_\odot = 20 \pm 4$ and $d(\log T_e)/dt = -0.028 \pm 0.003$ century^{-1} during the quiescent recovery phase for a cycle of any length up to at least 10^3 yr.

Further refinements of the calculations would seem to be worth pursuing, especially for the problematic stars of the highest luminosity, for which the past rates of mass loss, and hence the previous evolutionary histories, are still relatively uncertain.

We are grateful to F. J. Rogers for providing the OPAL opacity tables and to the referee for correcting an error. Our work was supported by the NASA Astrophysics Research Program.

REFERENCES

Abt, H. A. 1957, ApJ, 126, 138
Appenzeller, I. 1989, in Physics of Luminous Blue Variables, ed. K. Davidson, A. F. J. Moffat, & H. J. G. L. M. Lamers (Dordrecht: Kluwer), 195
Bisnovatyi-Kogan, G. S., & Nadyoshin, D. K. 1972, Ap&SS, 15, 353
Davidson, K. 1971, MNRAS, 154, 415
———. 1987, ApJ, 317, 760
de Groot, M. 1985, Irish Astron. J., 17, 263
de Jager, C. 1984, A&A, 138, 246
Feinstein, A., & Marraco, H. G. 1974, A&A, 30, 271
Gaposchkin, S. 1943, ApJ, 97, 166
Glatzel, W., & Kiriakidis, M. 1993, MNRAS, 263, 375
Gough, D. O., Ostriker, J. P., & Stobie, R. S. 1965, ApJ, 142, 1649
Hubble, E., & Sandage, A. 1953, ApJ, 118, 353
Humphreys, R. M., & Davidson, K. 1994, PASP, 106, 1025
Humphreys, R. M., Leitherer, C., Stahl, O., Wolf, B., & Zickgraf, F.-J. 1988, A&A, 203, 306
Hutsemékers, D. 1994, A&A, 281, L81
Iglesias, C. A., Rogers, F. J., & Wilson, B. G. 1992, ApJ, 397, 717
Kiriakidis, M., Fricke, K. J., & Glatzel, W. 1993, MNRAS, 264, 50
Lamers, H. J. G. L. M. 1989, in Physics of Luminous Blue Variables, ed. K. Davidson, A. F. J. Moffat, & H. J. G. L. M. Lamers (Dordrecht: Kluwer), 135
Lamers, H. J. G. L. M., & de Groot, M. J. H. 1992, A&A, 257, 153
Lamers, H. J. G. L. M., & Fitzpatrick, E. L. 1988, ApJ, 324, 279
Lamers, H. J. G. L. M., & Leitherer, C. 1993, ApJ, 412, 771
Langer, N., Hamann, W.-R., Lennon, M., Najarro, F., Pauldrach, A. W. A., & Puls, J. 1994, A&A, 290, 819
Leitherer, C., Appenzeller, I., Klare, G., Lamers, H. J. G. L. M., Stahl, O., Waters, L. B. F. M., & Wolf, B. 1985, A&A, 153, 168
Maeder, A. 1989, in Physics of Luminous Blue Variables, ed. K. Davidson, A. F. J. Moffat, & H. J. G. L. M. Lamers (Dordrecht: Kluwer), 15
Nieuwenhuijzen, H., & de Jager, C. 1990, A&A, 231, 134
Pauldrach, A. W. A., & Puls, J. 1990, A&A, 237, 409
Percy, J. R., et al. 1988, A&A, 191, 248
Pigott, E. 1786, Phil. Trans. R. Soc. London, 76, 189
Rogers, F. J., & Iglesias, C. A. 1992, ApJS, 79, 507
Rosino, L., & Bianchini, A. 1973, A&A, 22, 453
Sharov, A. S. 1975, in IAU Symp. 67, Variable Stars and Stellar Evolution, ed. V. E. Sherwood & L. Plaut (Dordrecht: Reidel), 275
———. 1990, Soviet Astron., 34, 364
Spoon, H. W. W., de Koter, A., Sterken, C., Lamers, H. J. G. L. M., & Stahl, O. 1994, A&AS, 106, 141
Stothers, R. B., & Chin, C. w. 1983, ApJ, 264, 583
———. 1993, ApJ, 408, L85 (SC93)
———. 1994, ApJ, 426, L43 (SC94)
van Genderen, A. M. 1979, A&AS, 38, 381
———. 1989, A&A, 208, 135
van Genderen, A. M., de Groot, M. J. H., & Thé, P. S. 1994, A&A, 283, 89
Whitelock, P. A., Feast, M. W., Koen, C., Roberts, G., & Carter, B. S. 1994, MNRAS, 270, 364
Wolf, B. 1989, A&A, 217, 87
Wolf, B., & Stahl, O. 1982, A&A, 112, 111
———. 1990, A&A, 235, 340